SPECTRAL ELEMENT DISCONTINUOUS GALERKIN SIMULATIONS FOR WAKE POTENTIAL CALCULATIONS: NEKCEM*

Misun Min†, Paul F. Fischer, MCS, ANL, Argonne, IL 60439, USA
Yong-Chul Chae, APS, ANL, Argonne, IL 60439, USA

Abstract

In this paper we present high-order spectral element discontinuous Galerkin simulations for wake field and wake potential calculations. Numerical discretizations are based on body-conforming hexagonal meshes on Gauss-Lobatto-Legendre grids. We demonstrate wake potential profiles for cylindrically symmetric cavity structures in 3D including the cases for linear and quadratic transitions between two cross sections. Wake potential calculations are carried out on 2D surfaces for various bunch sizes.

INTRODUCTION

We have developed a large scale computational code, NEKCEM [5], for computing wake fields and wake potentials [1, 2] in 3D structures. NEKCEM employs a high order numerical scheme, especially spectral element discontinuous Galerkin method [3, 4]. It features accurate and efficient computations with high-performance in parallel.

FORMULATIONS

The governing equations to study beam dynamics and numerical discretizations in space and time are discussed. Formulations are used in a mixed form with cartesian and cylindrical coordinates for the sake of convenience.

Maxwell's Equations

$$\mu\frac{\partial H}{\partial t} = -\nabla\times E, \quad \epsilon\frac{\partial E}{\partial t} = \nabla\times H - J \tag{1}$$

$$\nabla\cdot E = \frac{\rho}{\epsilon}, \quad \nabla\cdot H = 0 \tag{2}$$

where the current source J is defined for an on-axis Gaussian beam moving in z direction

$$J = ce_z\rho(r)\rho(z-ct), \quad \rho(z) = \frac{1}{\sigma_z\sqrt{2\pi}}e^{\left(-\frac{z^2}{2\sigma_z^2}\right)} \tag{3}$$

Conservation Form

We re-write the equation (1) into a conservation form

$$Q\frac{\partial q}{\partial t} + \nabla\cdot F(q) = 0 \tag{4}$$

by defining

$$q = (H_x, H_y, H_z, E_x, E_y, E_z)^T \tag{5}$$

$$Q = diag(\mu,\mu,\mu,\epsilon,\epsilon,\epsilon). \tag{6}$$

The flux $F(q)$ has the following form:

$$\begin{bmatrix} 0 & E_z & -E_y & 0 & -H_z & H_y \\ -E_z & 0 & E_x & H_z & 0 & -H_x \\ E_y & -E_x & 0 & -H_y & H_x & 0 \end{bmatrix}^T \tag{7}$$

Numerical Discretizations

We approximate solutions to the Maxwell's equations in the computational domain Ω as a set of bodyconforming nonoverlapping hexagonal meshes Ω^e. We define local solution $\mathbf{q_N}$ on each Ω^e as

$$\mathbf{q_N}(x,t) = \sum_{j=0}^{N} q_j(t)L_j(x) \tag{8}$$

where $q_j(t)$ is the solution at N grid points x_j on Ω^e, and $L_j(x)$ is the three dimensional Legendre Lagrange interpolation polynomial associated with the N-nodes [3]. We seek the local solutions $\mathbf{q_N}$

$$\left(Q\frac{\partial \mathbf{q_N}}{\partial t} + \nabla\cdot F(\mathbf{q_N}), \phi\right)_{\Omega^e} = (\hat{n}\cdot[F-F^*], \phi)_{\partial\Omega^e} \tag{9}$$

where the local discontinuous test function is $\phi = L_i(x)$ and the numerical fluxes F^* are defined as in [4].

We use the fourth order Runge-Kutta method for time integration.

Initial Conditions

To describe the electromagnetic fields at the presence of the Gaussian beam for the initial time step, we first solve the Poisson equation in two dimensions at the cross section of the initial beam position

$$\nabla^2\Phi^{2D}(r) = -\frac{\rho^{2D}(r)}{\epsilon} \tag{10}$$

and get the two-dimensional electric field at the cross section

$$E^{2D} = -\nabla\Phi^{2D}(r) \tag{11}$$

Then, an initial electric field E in three dimensions is assigned along the z-direction using the two-dimensional electric field E^{2D} scaled by the initial Gaussian distribution $\rho(z)$ as

$$E(r,z) = E^{2D}(r) * \rho(z) \tag{12}$$

* Work supported by the U.S. Dept. of Energy under Contract DE-AC02-06CH11357.

† mmin@mcs.anl.gov

Boundary Conditions

We apply uniaxial perfectly matched layer (UPML) [6] in z-direction, and perfectly electric conducting (PEC) boundary [4] in radial direction.

UPML formulations are defined in 3D as follows:

$$\frac{\partial H_z}{\partial y} - \frac{\partial H_y}{\partial z} = \frac{\partial D_x}{\partial t} + \frac{1}{\epsilon}\sigma_y D_x \quad (13)$$

$$\frac{\partial H_x}{\partial z} - \frac{\partial H_z}{\partial x} = \frac{\partial D_y}{\partial t} + \frac{1}{\epsilon}\sigma_z D_y \quad (14)$$

$$\frac{\partial H_y}{\partial x} - \frac{\partial H_x}{\partial y} = \frac{\partial D_z}{\partial t} + \frac{1}{\epsilon}\sigma_x D_z \quad (15)$$

where $\sigma_x = -(x/d)^m(m+1)\ln(R)/2\eta d$, denoting d, x, m, R, and η for PML size, the PML depth, polynomial grading, reflection error, and impedance, respectively. Within UPML, the components of E are updated by

$$\epsilon\left[\frac{\partial E_x}{\partial t} + \frac{\sigma_z}{\epsilon}E_x\right] = \frac{\partial D_x}{\partial t} + \frac{\sigma_x}{\epsilon}D_x \quad (16)$$

$$\epsilon\left[\frac{\partial E_y}{\partial t} + \frac{\sigma_x}{\epsilon}E_y\right] = \frac{\partial D_y}{\partial t} + \frac{\sigma_y}{\epsilon}D_y \quad (17)$$

$$\epsilon\left[\frac{\partial E_z}{\partial t} + \frac{\sigma_y}{\epsilon}E_z\right] = \frac{\partial D_z}{\partial t} + \frac{\sigma_z}{\epsilon}D_z \quad (18)$$

A similar formula is defined for the components of H to update in UPML. In our simulations we apply UPML only in x-direction by choosing $\sigma_y = \sigma_z = 0$.

PEC boundary conditions are assigned at the boundaries in radial direction satisfying

$$\hat{n} \times E = \hat{n} \cdot H = 0. \quad (19)$$

COMPUTATIONAL RESULTS

We show the performance of NEKCEM and and demonstrate the wake potential profiles for beam dynamics on various cavity structures.

Performance

To demonstrate the performance of NEKCEM, we compute the case with standing wave solutions for the Maxwell's equations with periodic boundaries on a cube mesh. Computations are performed with 32 processors on Jazz at ANL for the computational sizes by increasing the numbers of meshes and the degree of polynomials. Figure 1 shows CPU time vs. degree of freedom and errors vs. degree of freedom for different degrees of polynomials. It shows that CPU time increases linearly depending on the degree of freedom, but not being dominated by the increases of the degrees of the polynomials. Errors are much smaller with higher degree of polynomial for a fixed amount of grids. This implies that one can obtain better efficiency and accuracy with the high order method we presented in this paper.

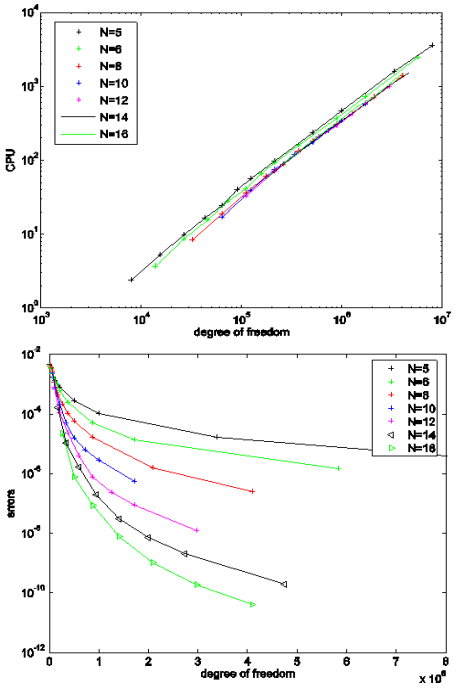

Figure 1: Performance with 32 processors on Jazz/ANL. CPU time vs. degree of freedom (up); Errors in log scale vs. degree of freedom (down).

Wake Potentials

Figure 2 shows electric field amplitude using contour lines on a half half side of a pillbox mesh with circle cross section radius $r = 1$ and $r = 2$. The wake potential calculations are carried out on the 2D surface at r=1 which is the size of Wake potential profiles show good agreement with ABCI results. Figure 3 shows meshes for the cavities with circle cross sections with radius changes from r=1 up to r=2. figure 4 shows wake potential calculations carried out on the 2D surface at r=1 which is the size of radius for the outgoing tube on the sides. The wake potential profiles for the cases with linear and quadratic transitions shows reasonable profiles depending the changes of the bunch sizes $\sigma_z = 0.25, 0.5, 0.75, 1.0$ for a fixed $\sigma_r = 0.1$.

CONCLUSIONS

We discussed spectral element discontinuous Galerkin method applied to beam simulations for three-dimensional cylindrical cavities with linear and quadratic transitions between circle cross sectons. The wake potential calculations show resonable profiles depending the variation of bunch sizes. We are currently tracking 1ps beam moving through meter scale cavities with linear and quadratic transitions between different sizes of elliptic cross sections. Rigorous comparisons on the wake potential calculations with other existing codes will be presented in a later paper.

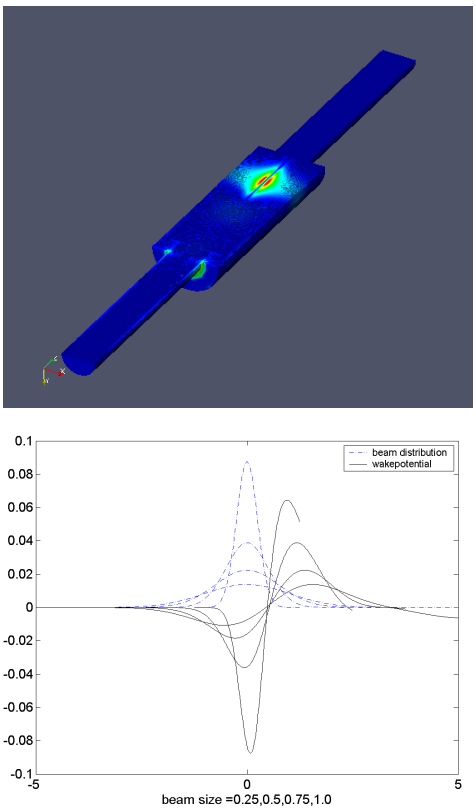

Figure 2: Contour lines of the electric field in amplitude on a half side of a pillbox mesh with circle cross section radius $r = 4$ and $r = 2$ (up). Wake potential on the surface at $r = 1$ for $\sigma_z = 0.25, 0.5, 0.75, 1.0$ and $\sigma_r = 0.1$ (down).

REFERENCES

[1] Y.C. Chae, "Horizontal Coupling Impedance of the APS Storage Ring", Proc. 2003 PAC (2003), p.3011.

[2] Y.H. Chin, "User's Guide for ABCI Version 9.4 and Introducing the ABCI Windows Application Package", KEK Report (2005) 2005-06.

[3] M.O. Deville, P.F. Fischer, and E.H. Mund, "High Order Methods for Incompressible Fluid Flow", Cambridge University Press (2002).

[4] J.S. Hesthaven and T. Warburton,"Nodal High Order Methods on Unstructured Grids - I. Time-Domain Solution of Maxwell's Equations", Journal of Computational Physics, 101 (2002), p.186.

[5] M.S. Min and P.F. Fischer, "NEKCEM", MCS/ANL, http://mercurial.mcs.anl.gov/nekcem/

[6] A. Taflov and S.C. Hagness, "Computational Electromagnetics: The Finite-Difference Time Domain Method", Artech House, 3rd Edition (2005).

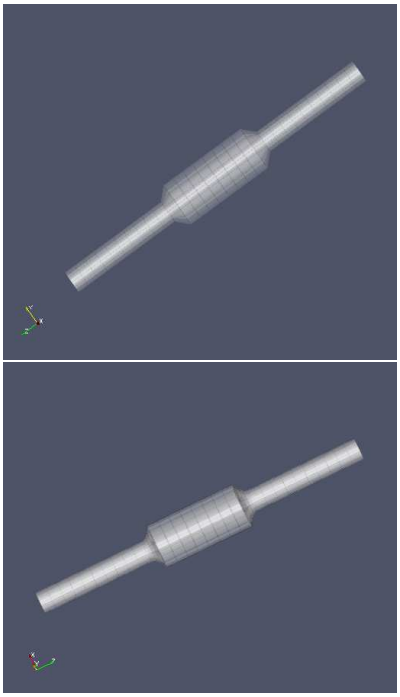

Figure 3: Meshes with circle cross sections with linear (up) and quadratic (down) transitions: tube radius is $r = 1$ for the outgoing tubes on sides.

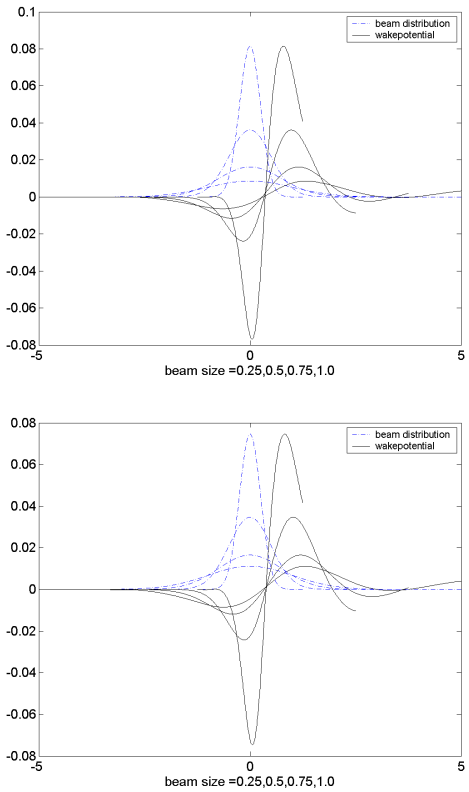

Figure 4: Wake potentials on the surface at $r = 1$ for $\sigma_z = 0.25, 0.5, 0.75, 1.0$ and $\sigma_r = 0.1$ on the meshes (shown in Figure 3) with linear (up) and quadratic (down) transitions.